JOURNAL OF GEOPHYSICAL RESEARCH: ATMOSPHERES, VOL. 118, 5304–5318, doi:10.1002/jgrd.50468, 2013

Evaluation of ECMWF's soil moisture analyses using observations on the Tibetan Plateau

Z. Su,[1] P. de Rosnay,[2] J. Wen,[3] L. Wang,[1] and Y. Zeng[1]

Received 20 November 2012; revised 24 March 2013; accepted 4 May 2013; published 13 June 2013.

[1] An analysis is carried out for two hydrologically contrasting but thermodynamically similar areas on the Tibetan Plateau, to evaluate soil moisture analysis based on the European Centre for Medium-Range Weather Forecasts (ECMWF) previous optimum interpolation scheme and the current point-wise extended Kalman filter scheme. To implement the analysis, this study used two regional soil moisture and soil temperature networks (i.e., Naqu and Maqu) on the Tibetan Plateau. For the cold-semiarid Naqu area, both ECMWF soil moisture analyses significantly overestimate the regional soil moisture in the monsoon seasons. For the cold-humid Maqu network area, the ECMWF products have comparable accuracy as reported by previous studies in the humid monsoon period. The comparisons were made among the liquid soil moisture analysis from ECMWF, the ground station's measurements and the satellite estimates from the Advanced Scatterometer sensor. The results show reasonable performances of the ECMWF soil moisture analyses (i.e., both optimum interpolation and extended Kalman filter products) and the Advanced Scatterometer level 2 products, when compared to the in situ measurements.

Citation: Su, Z., P. de Rosnay, J. Wen, L. Wang, and Y. Zeng (2013), Evaluation of ECMWF's soil moisture analyses using observations on the Tibetan Plateau, *J. Geophys. Res. Atmos.*, *118*, 5304–5318, doi:10.1002/jgrd.50468.

1. Introduction

[2] Understanding the physics and dynamics of soil moisture is crucial to understanding the role of the hydrological cycle in the climate system [*Milly and Dunne*, 1994; *Polcher*, 1995; *Drusch*, 2007; *Basalmo et al*., 2009; *de Rosnay et al*., 2009]. With increasing evidence of climate change, it becomes more urgent to quantify the critical role of soil moisture in climate, because the response of the hydrological cycle to global warming is expected as far reaching [*Bengtsson*, 2010]. Quantification of trends and variability in global soil moisture can contribute to better understanding the feedback between the water cycle and climate. Although it is easy to observe soil moisture dynamics at the local scale, it is challenging to translate this point scale understanding to natural landscapes due to the lack of understanding of soil moisture variability at larger spatial scales. Models [*Dirmeyer et al*., 2004], satellite remote sensing [e.g., *Wagner et al*., 2003; *Njoku et al*., 2003; *Wen and Su*, 2003a, 2003b; *Wen et al*., 2003; *Owe et al*., 2008], and land data assimilation [*Drusch et al*., 2005; *Yang et al*., 2009; *Qin et al*., 2009; *Tian et al*., 2009] are necessary tools to produce spatiotemporally consistent soil moisture information. However, all these estimates need validations for their consistencies at a variety of representative sites with intensive soil moisture measurements before their use in quantifying the feedback between the water cycle and climate should be commissioned.

[3] Soil moisture analysis at the European Centre for Medium-Range Weather Forecasts (ECMWF) aims to represent spatiotemporally consistent soil moisture information, served as land surface initialization for numerical weather prediction models [*de Rosnay et al*., 2012a]. The optimum interpolation (OI) scheme is the previous operational soil moisture analysis scheme at ECMWF [*Mahfouf et al*., 2000], using the increments of the screen-level parameters analysis as input. The current soil moisture analysis scheme is a point-wise extended Kalman filter (EKF) with the same screen-level parameters analysis. Both schemes provide similar soil moisture analysis, due to the use of screen-level proxy observations [*Drusch et al*., 2009; *de Rosnay et al*., 2012b]. However, the current EKF scheme opens up the possibility to combine remote sensing data (e.g., satellite derived soil moisture data) with screen-level proxy observations, and it better constrains the soil moisture fields. *De Rosnay et al*. [2012b] also investigated the impact of including the Advanced Scatterometer (ASCAT) soil moisture data on the ECMWF land surface analysis system, and found a neutral impact on both soil moisture analysis and screen-level parameters. That study implies that further improvements in the ASCAT soil moisture products and bias corrections are expected to enhance the impact of using ASCAT in the soil moisture analysis.

[1]Faculty of Geo-Information Science and Earth Observation (ITC), University of Twente, Enschede, the Netherlands.
[2]European Centre for Medium-Range Weather Forecasts, Reading, United Kingdom.
[3]Cold and Arid Regions Environmental and Engineering Research Institute, Chinese Academy of Sciences (CAREERI/CAS), Lanzhou, China.

Corresponding author: Z. (Bob) Su, Faculty of Geo-Information Science and Earth Observation (ITC), University of Twente, P.O. Box 217, 7500 AE, Enschede, the Netherlands. (z.su@utwente.nl)

2169-897X/13/10.1002/jgrd.50468

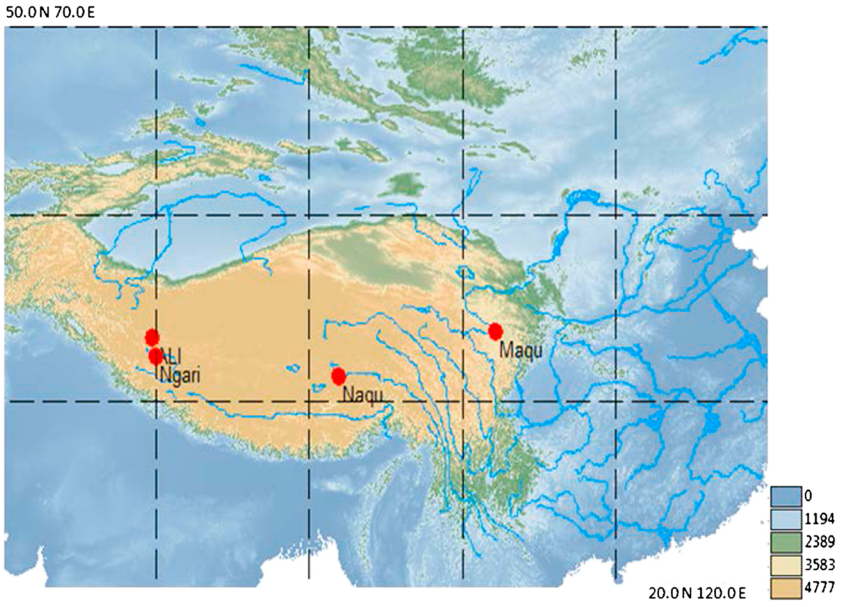

Figure 1. Location of the three regional networks of the Tibetan Plateau soil moisture and soil temperature Observatory (Tibet-Obs). Data from the Naqu and the Maqu networks are used in this study.

[4] Recently, *Su et al*. [2011] have carried out a thorough validation of several satellite soil moisture estimates (e.g., including ASCAT level 2, ASCAT-L2, soil moisture data). The uncertainties of those global coarse resolution soil moisture products were quantified and characterized, using the in situ measurements from the Tibetan Plateau soil moisture and soil temperature observatory (Tibet-Obs). The ASCAT-L2 data with quantified uncertainties enhances its operational use on the Tibetan Plateau [*Su et al*., 2011].

[5] In this paper, using the in situ measurements from the Tibet-Obs and the operational ASCAT-L2 data product, we aim to evaluate the ECMWF's previous operational OI soil moisture scheme (ECMWF-Oper-OI), which was used in the ECMWF interim reanalysis (ERA-interim from 1979 onwards) [*Dee et al*., 2011], and the current EKF soil moisture scheme. The EKF soil moisture product includes the soil moisture analysis using the screen-level proxy observation only and the analysis using both the proxy observation and the ASCAT data (ECMWF-*H-SAF*) [*Albergel et al*., 2012a, 2012b; *de Rosnay et al*., 2012b]. This study uses three numerical experiments with different assimilation approaches, to illuminate the impact of the analysis scheme on analyzed soil moisture fields in the Tibetan Plateau. These include an Open Loop, i.e., without any soil moisture assimilation, OI and EKF approaches both using screen level observation only. This paper consists of a short introduction of the Tibet-Obs and the characteristics of the used data (section 2), a brief description of the ECMWF OI and EKF data assimilation systems and products used (section 3), an analysis of the ECMWF soil moisture products against the in situ measurements and the satellite data (section 4), and discussions and conclusion for future investigations (section 5).

2. The Tibet-Obs In Situ Soil Moisture and Soil Temperature Networks

[6] The Tibetan Plateau observatory of plateau-scale soil moisture and soil temperature (Tibet-Obs) consists of three regional-scale in situ reference networks (Figure 1), including the Naqu network in a cold-semiarid climate, the Maqu network in a cold-humid climate, and the Ngari network in a cold and arid climate. These networks provide a representative coverage of the different climate and land surface hydrometeorological conditions on the Tibetan Plateau. This paper will only use the operational Naqu and Maqu networks (data from the Ngari network are not available for the analyzed period). The following part of this section gives a brief description of the characteristics of the used data in this study, while detailed information for each network has been given by *Su et al*. [2011].

2.1. The Naqu Network in a Cold Semiarid Environment

[7] The Naqu study area is located in the Naqu basin with a smooth terrain with rolling hills at an average elevation of 4500 m above mean sea level (a.s.l). The study area has soils with high saturated hydraulic conductivity positioned on top of an impermeable rock formation (or permafrost layer) resulting in rapid surface runoff and accumulations in local depressions forming lakes and wetlands in the monsoon season (usually from June to September). The land cover in the higher parts of the study area can be characterized as grasslands consisting of prairie grasses and mosses and wetland in the lower areas [*van der Velde et al*., 2009; *van der Velde and Su*, 2009; *van der Velde et al*., 2008; *van der Velde*, 2010]. In the winter period from November to April, there exists a stable frozen soil. The Naqu soil moisture and soil temperature network was installed around the Naqu climate station (31°22 N, 91°53 E) located about 25 km southwest of Naqu City initially as a part of Global Energy and Water cycle Experiment supported field campaigns [*Ma et al*., 2003, 2006, 2007]. Continuous measurements are made of water and energy exchanges between the land surface and atmosphere at this station, including atmospheric variables at different heights, radiation, turbulent heat

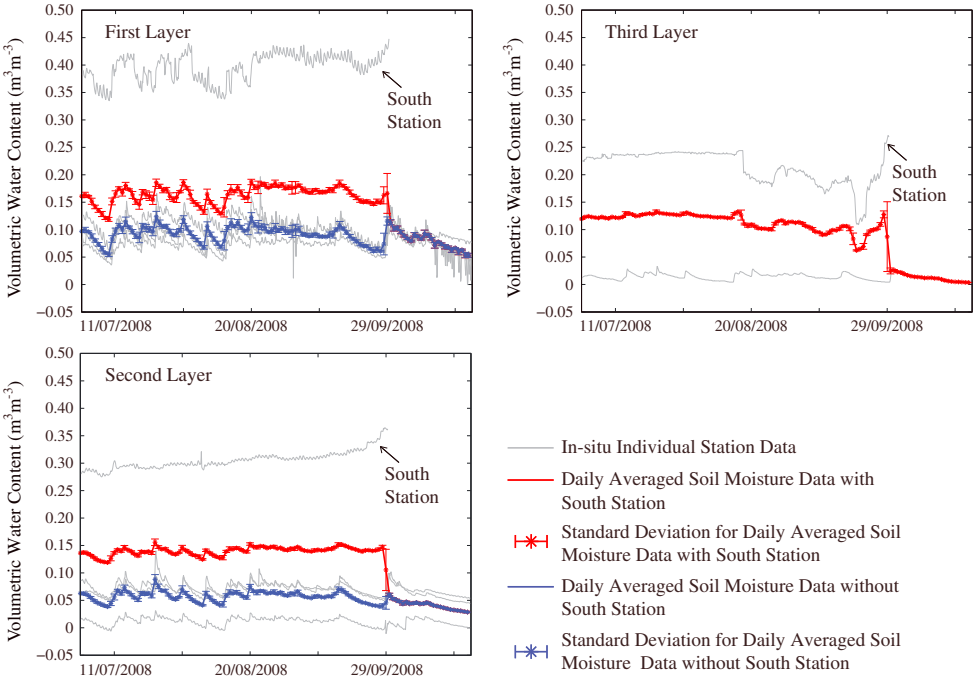

Figure 2. The comparison between the individual station observations and the averaged soil moisture data for Naqu network during 1 July 2008 to 23 October 2008.

fluxes, and soil moisture and soil temperature at different depths [e.g., *Ma et al.*, 2007; *van der Velde et al.*, 2009].

[8] The Naqu soil moisture and soil temperature stations were placed within 10 km north, south, west, and east of the Naqu climate station with an additional one installed at Naqu climate station itself (i.e., in total 5 stations) for comparison purpose with the existing instrumentation. Grasslands dominate the land cover at the north, west, and east Naqu stations and south station is located in a wetland. The instrumentation used for these stations consists of EM5b data loggers and 0.10 m long ECH_2O impedance probes both manufactured by Decagon Devices. At each station, probes have been installed horizontally at depths of 2.5, 7.5, 15.0, 30.0, and 60.0 cm with a sampling interval set at 3 h in the data analyzed here. The accuracy of the in situ measurement is reported, by comparison with gravimetrically determined and impedance probe soil moisture, as a root mean square difference (RMSD) of 0.029 $m^3 \cdot m^{-3}$ [*van der Velde*, 2010].

[9] The averaged network-scale soil moisture is derived from the daily averages of the 3-hourly measurements at each depth for each station. Because the ECMWF model layers do not correspond to the in situ measurements depth directly, we assign the average of in situ measurements at the 2.5 and 7.5 cm to the first model layer of 0–7 cm, the average of 15 and 30 cm to the second layer of 7–28 cm, and in situ measurement at 60 cm to the third layer of 28–100 cm, respectively. Figure 2 shows the comparison between the individual station observation and the averaged layered soil moisture data for the Naqu network. The South Station is highlighted due to its "abnormal" behavior compared to other stations. The main reason for the high volumetric content in the South Station is due to the installation of the probe at the edge of a wetland. The daily soil moisture data for the Naqu network was averaged including and excluding the South Station data. It may be argued that, for the first and second layer, the averaged data excluding the "wet" data is more representative than that with the 'wet' data.

[10] Not all the sensors at all depths recorded data, because of the harsh environment in Naqu. For the first layer, all five stations provided data; for the second layer, there were four stations, and there were only two stations for the third layer. In this study, for the first layer and the second layer, the averaged data excluding the "wet" layer was used. The third layer data was discarded, because one is too "wet" and the other is too "dry." Even if the average of them may be representative of the Naqu network at the third layer, it is not suggested to be used in this study, due to the unknown uncertainties. The standard deviation of the daily averaged soil moisture data representing the error may rise by averaging the 3-hourly data in one day (e.g., temporal-error bars). *Su et al.*

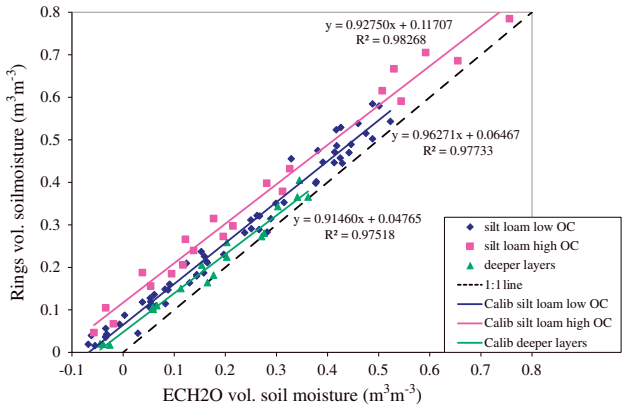

Figure 3. Calibration of ECH2O sensor in soils containing different organic matter content for Maqu network area.

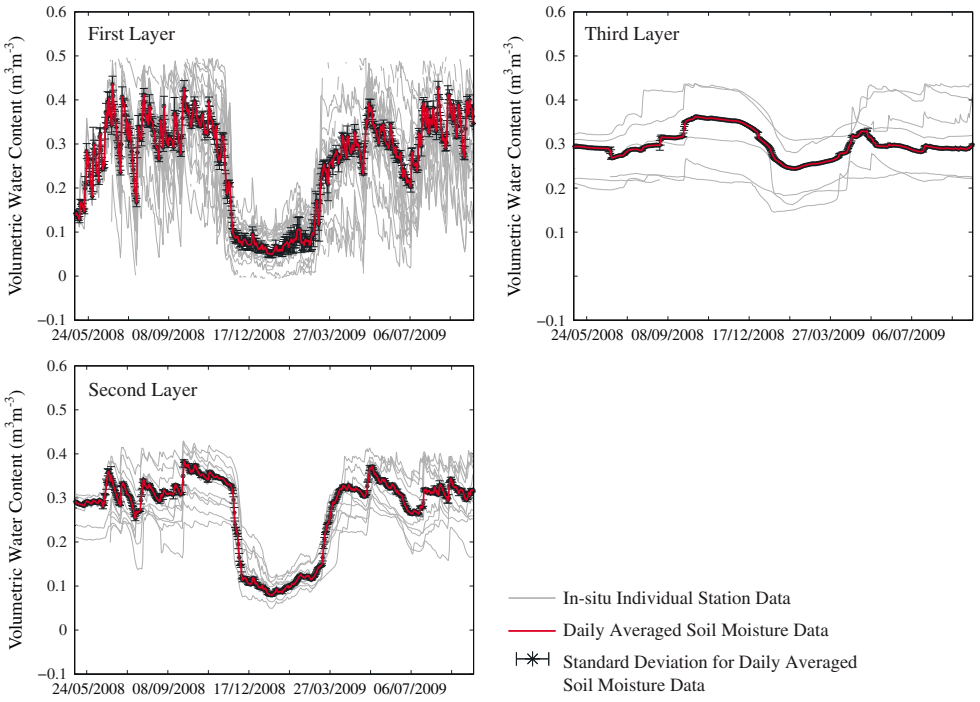

Figure 4. The comparison between the individual station observations and the averaged soil moisture data for Maqu network during 13 May 2008 to 27 September 2009.

[2011] and *van der Velde* [2010] had presented the detailed spatial-error analysis of the in situ data for Naqu Network.

2.2. The Maqu Network in a Cold and Humid Environment

[11] The Maqu soil moisture and soil temperature monitoring network, consisting of 20 stations and covering an area of approximately 40 km by 80 km, was installed in July 2008 in the water source region of the Yellow River to the south of Maqu County in Gansu province, China. The network is located at the northeastern edge of the Tibetan Plateau (33°30′–34°15′N, 101°38′–102°45′E) at the first major meander of the Yellow River. The network area covers the large valley of the river and the surrounding hills characterized by a uniform land cover of short grassland used for grazing. The elevation ranges between 3430 m and 3750 m a.s.l. including typical landscapes with hills, valleys, river, wetlands, grassland, and bare soil areas. Wetlands, with typically organic soils, characterize a large part of the valley, while silt loam soils can be found on the hills. According to the Koeppen Classification System, the climate at this site is defined as wet and cold, with dry winters and rainy summers due to the East Asia monsoon. More details for this network are given by *Dente et al.* [2009, 2011]. The stations continuously monitor the soil moisture and soil temperature at different depths (from 5 to 80 cm deep) at 15 min intervals.

[12] The capacitance EC-TM ECH_2O probe with three flat pins of 5.2 cm length is used to obtain volumetric soil moisture. The soil temperature is measured using a thermistor located on the same probe. The soil texture in most stations is quite homogeneous with silt loam at upper soil layers down to more than 40 cm depth. The main difference between the stations is organic matter content. The probes were calibrated gravimetrically to reduce the RMSD between the gravimetric moisture content and the probe measurements, from 0.06 to

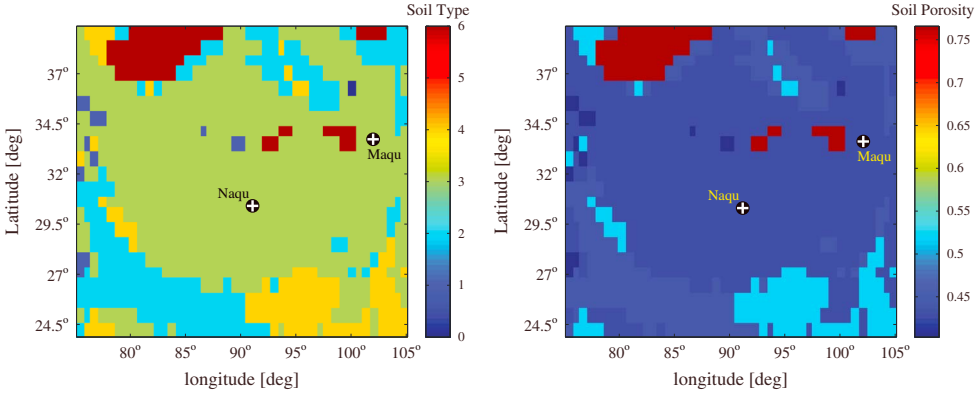

Figure 5. The soil type and soil porosity map adopted in HTESSEL for Tibetan Plateau area.

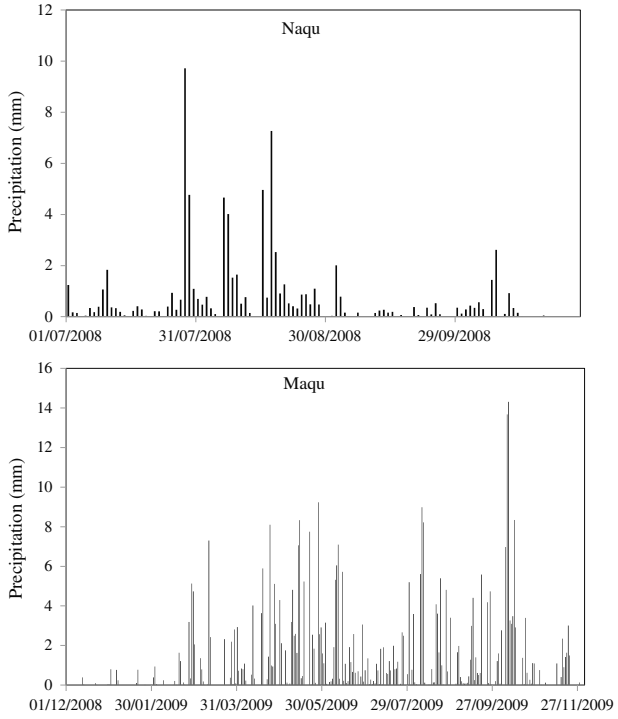

Figure 6. The forecasted precipitation products used for the Naqu and Maqu network results.

0.02 m^3m^{-3} (Figure 3). The values can be considered as the absolute accuracy at this network [*Dente et al*., 2009]. Figure 3 shows the calibration results of ECH2O sensor in soil containing different organic matter content, with high volume of which the soil saturation can reach around 0.8 m^3m^{-3}. This is identical to *Chen et al*.'s [2012] results. It is noticed that the negative value from the sensor, which occurred in the field when soil is frozen, has been calibrated as well. *Yoshikawa and Overduin* [2005] indicated that the calibrated Frequency Domain Reflectometry (FDR) sensor (e.g., ECH2O) can capture the freezing-thawing process with small absolute errors (<0.01 m^3m^{-3}), even if the actual water content is most likely lower than 0.01 m^3m^{-3} in the frozen soil during the coldest period of winter. *Van der Velde* [2010] has implemented the same kind of gravimetrical calibration for the sensors used in the Naqu network.

[13] For this network area, we assign the average of the in situ measurements at the 0.05 m to the first model layer of 0.0–0.07 m, the average of 0.20 and 0.40 m to the second layer of 0.07–0.28 m, and in situ measurement at 0.80 m to the third layer of 0.28–1.00 m, respectively. Figure 4 shows the comparison between the individual station observations and the average layered soil moisture data for the Maqu network. Not all stations in Maqu network were equipped with sensors at all depths. For the first layer, all 20 stations recorded data; for the second layer, there were 11 stations available; and there were only 5 stations available for the third layer. In this study, the averaged soil moisture at all the three layers were used in the analysis. The detailed explanations on the spatial-error analysis of the in situ data and the spatial distribution of stations for the Maqu network are referred to *Su et al*. [2011] and *Dente et al*. [2011].

3. Satellite Data and ECMWF Soil Moisture Products

3.1. Satellite Data (ASCAT-L2 and AMSR-E)

[14] The ASCAT-L2 data are retrieved from the European Organisation for the Exploitation of Meteorological Satellites (EUMETSAT). The ASCAT-L2 data are global coarse-resolution soil moisture data (25–50 km) derived from backscatter measurements acquired with the scatterometers onboard the MetOp satellite, with relative values scaled between 0 and 1 representing dry and saturation conditions, respectively [*Bartalis et al*., 2007; *Scipal et al*., 2008]. These satellite data are rescaled to volumetric soil moisture to be compatible with other satellite data and easy for comparison with the in situ measurements, using the soil database of the Food and Agriculture Organization (FAO) (2003) [*Reynolds et al*., 1999].

[15] The Advanced Microwave Scanning Radiometer (AMSR-E) products were retrieved from http//www.geo.vu.nl/~jeur/lprm/, which provides daily 0.25° (25 km) surface soil moisture and land surface temperature data from AMSR-E observations; the nighttime overpass products are used because the daytime overpass data have major uncertainties caused by temperature variations.

3.2. ECMWF Soil Moisture Products

[16] The ECMWF Integrated Forecasting System (IFS) includes a land surface analysis system independent of the upper air analysis [*Drusch and Viterbo*, 2007; *de Rosnay et al*., 2012a]. The soil moisture analysis implemented in 1999 at ECMWF used an optimum interpolation for more than 10 years until 2010, using air temperature and air humidity at 2 m height as proxy information to analyze soil moisture. However, this system was not flexible to include new types of data as those provided by satellites. An extended Kalman filter soil moisture analysis was developed [*Drusch et al*., 2009] and implemented in the operational surface analysis at ECMWF in November 2010 [*de Rosnay et al*., 2012b].

Table 1. ECMWF Soil Moisture Analyses Products Used in This Paper

Name	SM DA Approach	Assimilated Observations	Spatial Resolution (km)	Available Period
ECMWF-Oper-OI	OI	T2m, Rh2m	25	1 July 2008 to 23 October 2008 (Naqu)1 May 2008 to 23 September 2008 (Maqu)
ECMWF-H-SAF	EKF	T2m, Rh2m, ASCAT	25	1 July 2008 to 23 October 2008 (Naqu)1 May 2008 to 23 September (Maqu)
ECMWF-OL	No DA	None	80	1 December 2008 to 30 November 2009
ECMWF-OI	OI	T2m, Rh2m	80	1 December 2008 to 30 November 2009
ECMWF-EKF	EKF	T2m, Rh2m	80	1 December 2008 to 30 November 2009

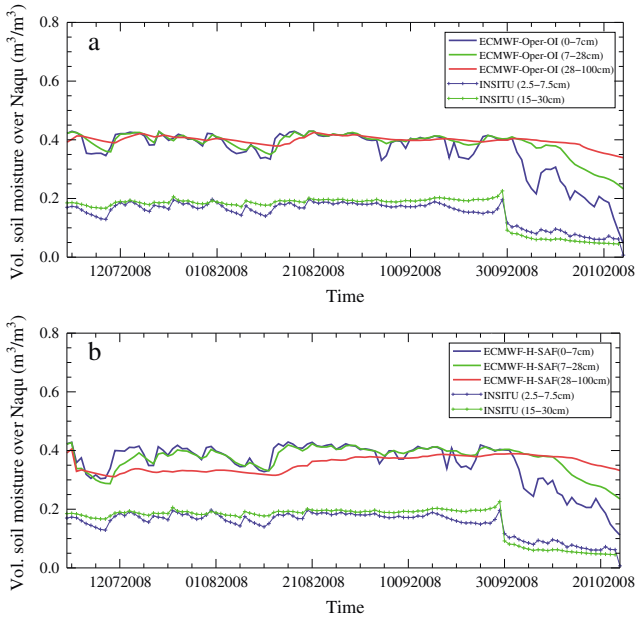

Figure 7. Soil moisture from (a) the ECMWF pervious operational run (ECMWF-Oper-OI, where the SM analysis uses the optimal interpolation method) and (b) the ECMWF-H-SAF numerical experiment (using the EKF soil moisture analysis with ASCAT data assimilation), compared to in situ measured soil moisture in the Naqu network area.

[17] The land surface analyses tasks are performed separately from the upper-air atmospheric analysis (4D-Var), both of which are used together as initial conditions for the first-guess forecast and the 10 day forecast. The analyses are produced twice daily based on two 12 h data assimilation windows, performed from 2100 to 0900 UTC and from 0900 to 2100 UTC. The land surface analyses include the analyses of screen-level parameters (2 m temperature and relative humidity), snow depth, soil moisture, soil temperature, and snow temperature. The screen-level parameter analysis is the first to be completed and is used as input for the soil moisture and snow analyses. The soil and snow temperature analyses, which rely on an OI approach, are completed after snow and soil moisture is finished. The analyzed surface variables generate feedback for the upper-air analysis of the next assimilation window, through their influence on the first-guess forecast that propagates information from one cycle to the next. The background-error covariance matrix and the observation-error matrix are set static, with diagonal terms composed of error variances. These terms are based on soil moisture standard deviation (σ_b= 0.01 $m^3 \cdot m^{-3}$) and screen-level parameter standard deviations (σ_T=2 K and σ_{RH}=10%), and the soil moisture perturbations were set to 0.01 $m^3 \cdot m^{-3}$ to get the most appropriate Jacobians of the observation operator [*de Rosnay et al*., 2012b; *Drusch et al*., 2009].

[18] In this paper, ECMWF operational soil moisture analysis based on the OI (ECMWF-Oper-OI) is evaluated with ground observations in 2008 and 2009. In addition, numerical experiments using the new EKF soil moisture analysis by assimilating ASCAT soil moisture data are carried out (ECMWF-H-SAF). This later product has been developed in the framework of the EUMETSAT Satellite Application Facility (SAF) in support of the operational hydrology and water management (H-SAF). Both ECMWF soil moisture analyses were produced at a 25 km resolution (T799). They contain four layers of volumetric soil moisture in $m^3 \cdot m^{-3}$, first layer (0–7 cm), second layer (7–28 cm), third layer (28–100 cm), and fourth layer (100–189 cm) below the ground surface, based on the land surface model used. The land surface model used in ECMWF surface analysis scheme is the Hydrology Tiled ECMWF Scheme for Surface Exchanges over Land (HTESSEL) [*Balsamo et al*., 2009]. The soil moisture and soil temperature analyses produced daily at 00UTC of the first three layers are analyzed.

[19] Hydrology Tiled ECMWF Scheme for Surface Exchanges over Land accounts for global soil texture, based on the FAO Digital Soil Map (2003). For each model grid box, dominant soil texture is used to define soil hydraulic properties. Figure 5 shows that the Naqu and Maqu stations share the same soil hydraulic properties in HTESSEL, which is defined as medium fine texture with the soil type value of "3." HTESSEL also accounts for vegetation subgrid-scale variability, based on Global Land Cover Characteristics data [*Balsamo et al*., 2009]. For the energy part, the soil energy budget follows a Fourier diffusion law, modified to take into account soil water freezing and thawing according to *Viterbo et al*. [1999], which is solved with a net ground heat-flux as the top boundary condition and zero flux as the lower boundary condition. For the hydrology part, with the top boundary condition of infiltration (e.g., due to precipitation) plus surface evaporation and the bottom boundary condition of free drainage, the subsurface water fluxes are determined by Darcy's law. The precipitation is a forecast product from the atmospheric part of ECMWF IFS. Figure 6 shows the precipitation used in this study, for Naqu and Maqu network. The vertical movement of water in the unsaturated zone of the soil matrix obeys the Richards equation for the volumetric water content and accounts for the root extraction by considering a sink term [*Viterbo and Beljaars*, 1995]. Each individual grid box is in energy and hydrological contact with one single atmospheric profile and one soil profile.

Table 2. The Naqu Network Area - Statistics of the ECMWF Operational Run (ECMWF-Oper-OI) and the ECMWF-H-SAF Numerical Experiment (Using the EKF Soil Moisture Analysis With ASCAT Data Assimilation) Compared to the In Situ Measured Soil Moisture ($m^3 \cdot m^{-3}$)

Layer Depth	RMSD (ECMWF-Oper-OI)	MD (ECMWF-Oper-OI)	*R* (ECMWF-Oper-OI)	RMSD (ECMWF-H-SAF)	MD (ECMWF-H-SAF)	*R* (ECMWF-H-SAF)
ECMWF first layer (0–7 cm) in situ (2.5–7.5 cm)	0.215	0.210	0.918	0.211	0.207	0.913
ECMWF second layer (7–28 cm) in situ (15–30 cm)	0.229	0.226	0.722	0.217	0.212	0.550

Shown are root mean square difference (RMSD), bias (MD), and correlation coefficient (*R*).

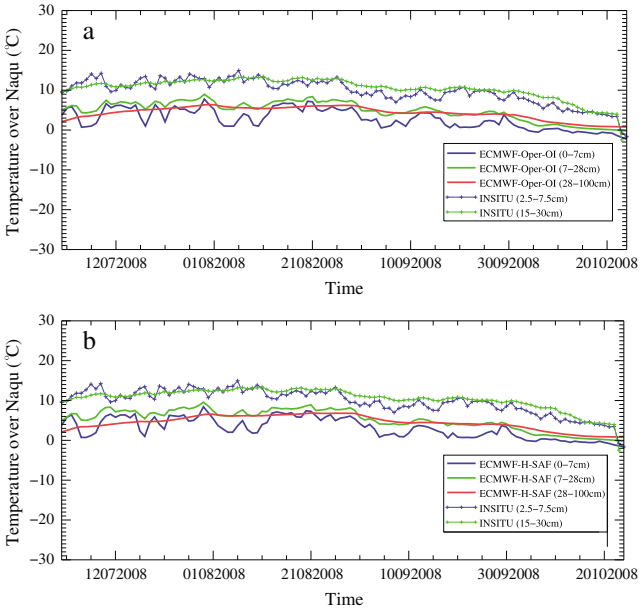

Figure 8. Same as Figure 7 but for soil temperature.

[20] *Albergel et al*. [2012a, 2012b] provided an evaluation of the ECMWF-H-SAF, together with ASCAT and the ESA Soil Moisture and Ocean Salinity satellite soil moisture products, against more than 200 surface soil moisture stations across the world. They showed good performances of the assimilated and remotely sensed products to capture soil moisture dynamics at seasonal and subseasonal time scales. In addition to the ECMWF-Oper-OI and the ECMWF-H-SAF, three experiments were conducted from December 2008 to November 2009, at lower resolution (80 km) to purely evaluate the impact of the data assimilation approach on the soil moisture analysis performance. Table 1 summarizes the experiment setup. The two experiments ECMWF-OI and ECMWF-EKF were evaluated by *de Rosnay et al*. [2012b]. They showed that compared to ECMWF-OI, the ECMWF-EKF soil moisture analysis improves both soil moisture and lowest level atmospheric parameters forecasts.

4. Results

4.1. Results of ECMWF-Oper-OI and ECMWF-H-SAF at Naqu Network

[21] The computed soil moisture (e.g., only liquid water content) of the first three layers by the ECMWF-Oper-OI system and the ECMWF-H-SAF system are plotted with the measured soil moisture values at Naqu network in Figures 7a and 7b, respectively, for the monsoon to winter transition period (from 1 July 2008 to 23 October 2008). The in situ soil moisture is a simple average at the available stations, which is considered justified for the purpose of comparison with coarse model grid data (~25 km) (see Figure 2). The ECMWF soil moisture product accounts for the water and heat transport in frozen soil, where the soil moisture includes liquid and solid phases (i.e., ice). During the winter period, the in situ measurements cannot provide the total water content (i.e., liquid and solid) when the soil is frozen, due to the measurement principle the sensor adopted. To do a fair comparison between the ECMWF soil moisture product and the in situ measurement, only the liquid water content estimates from the ECMWF soil moisture analysis were used.

[22] It is observed that the first and second model layers follow the gradual decreasing of soil moisture at the Naqu network area, in particular to the temporal variations caused by precipitation (see Figure 6). However, there are dramatic differences in the magnitudes. Both the ECMWF-Oper-OI and ECMWF-H-SAF products have a mean value of 0.40 $m^3\,m^{-3}$ before October when the winter sets in, overestimating the areal mean of less than 0.20 $m^3\,m^{-3}$ in the in situ measurements.

[23] At least two issues can be accounted for the overestimation: (1) the land surface analysis system used, and (2) the observations. The observation at this network has been calibrated using gravimetric measurements [*van der Velde*, 2010]. The main deviation may be attributed to the land surface analysis system used, which includes the initialization, boundary conditions, soil properties (e.g., including land cover type), and the soil physics process and so on. Considering the soil layer depths between the observation and the ECMWF product are comparable, the relatively high correlations (see Table 2) between them indicate that the temporal variations of the in situ observations can be captured by the soil moisture analysis. This means that the boundary conditions and the soil physics process cannot be significant factors accounting for the overestimations. The model first guess soil moisture fields in the land surface system may be the main cause for the overestimation because the dramatic differences are related to the land surface model soil moisture range.

[24] The main deviation may be as well related to soil texture, which determines the soil hydraulic properties, at this network. From Figure 5, there is no difference in soil texture for almost the entire Tibetan Plateau (e.g., the medium fine soil) in the HTESSEL model. For the Naqu network, it means that the volumetric water content at saturation is 0.43 $m^3\,m^{-3}$, at wilting point is 0.133 $m^3\,m^{-3}$, and at field capacity is 0.382 $m^3\,m^{-3}$; and, the saturated hydraulic conductivity is $5.5 \times 10^{-7}\,m\,s^{-1}$. However, the local sampled soil texture derived from *Chen et al*. [2012] suggested that

Table 3. The Naqu Network Area - Statistics of the ECMWF Operational Run (ECMWF-Oper-OI) and the ECMWF-H-SAF Numerical Experiment (Using the EKF Soil Moisture Analysis With ASCAT Data Assimilation) Compared to the In Situ Measured Soil Temperature (°C)

Layer Depth	RMSD (ECMWF-Oper-OI)	MD (ECMWF-Oper-OI)	*R* (ECMWF-Oper-OI)	RMSD (ECMWF-H-SAF)	MD (ECMWF-H-SAF)	*R* (ECMWF-H-SAF)
ECMWF first layer (0–7 cm) in situ (2.5–7.5 cm)	7.34	−6.90	0.63	7.07	−6.63	0.65
ECMWF second layer (7–28 cm) in situ (15–30 cm)	5.71	−5.57	0.86	5.39	−5.23	0.87

Shown are root mean square difference (RMSD), bias (MD), and correlation coefficient (*R*).

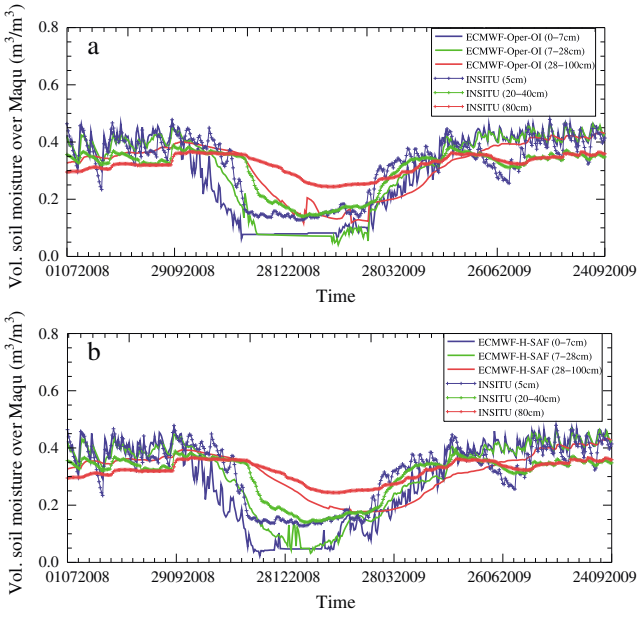

Figure 9. Soil moisture from (a) the ECMWF operational run (ECMWF-Oper-OI, where the SM analysis uses the OI) and (b) the ECMWF-H-SAF numerical experiment (using the EKF soil moisture analysis with ASCAT data assimilation), compared to in situ measured soil moisture at the Maqu network area.

the volumetric water contents at saturation, wilting point, and field capacity are 0.44, 0.058, and 0.113 $m^3\,m^{-3}$, respectively; and, the saturated hydraulic conductivity is 2.8×10^{-5} $m\,s^{-1}$. The model hydraulic conductivity is much smaller than the local sampled one, which means slower water transport in the model than in the field. This causes subsequently the higher volumetric water content in the model than in the field, which can explain the overestimation in ECMWF results. The discrepancy appears to increase with the increase of soil depth from the first to the second layer, resulting in a lower correlation coefficient in the second layer than the first layer (Table 2).

[25] The assimilation of the ASCAT-L2 data (ECMWF-H-SAF in Table 2 and Figure 7b) does not appear to improve the statistics or the magnitudes of the model estimates of the first and second layer, although a decrease of about 0.01 $m^3 \cdot m^{-3}$ can be observed for the second layer, compared to the ECMWF-Oper-OI analysis. This is explained by the fact that the EKF analysis increments are much reduced compared to the OI in the deep soil moisture layers [*de Rosnay et al.*, 2012b]. The OI system uses the same coefficients for all the soil layers, without accounting for distinct values for the different soil layers. Therefore, in this area, where positive increments are computed, the OI tends to add too much water at depth. In contrast, the Jacobians in the EKF are computed dynamically and separately for each soil layer, such that the EKF analysis accounts for different coupling strengths between soil and air parameters at 2 m height. Because the coupling strength decreases at depth, the EKF increments are much reduced at depth compared to those of the OI. In addition to the screen level parameters, the EKF also uses ASCAT data. However, the impact of using ASCAT data is very limited, compared to the EKF impact itself. It is mainly due to that the ASCAT data delivered through EUMETCAST until 2010 is very noisy. The recalibrated version to be delivered by EUMETSAT is expected to improve the efficiency of ASCAT data assimilation. Another point that needs attention is that the ASCAT data used in ECMWF land surface analysis system have been rescaled to the model soil moisture using a CDF matching method [*Scipal et al.*, 2008]. The matching corrects observation biases against model output of surface soil moisture and results in only assimilating the observed ASCAT soil moisture variability.

[26] In a previous study, *Su et al.* [2011] reported that the ASCAT-L2 data systematically and significantly overestimated the surface soil moisture in this network area. The average soil moisture in this area is usually very low in the monsoon period. Because of its frozen conditions in winter, the soil moistures measured with the in situ probes are practically identical to those of the dry soil in winter. In addition, it was the first time to observe such a big uncertainty in cold and semiarid conditions, confirming previous findings [e.g., *Dorigo et al.*, 2010] stating that the change detection algorithm is unreliable in arid conditions. From this study, it seems that ASCAT-L2 data do not contain significant information to improve the dynamics or the magnitudes in soil moisture estimates in the ECMWF land surface analysis system. On the other hand, the ECMWF land surface system may need further developments to enhance its capacity to use remote sensing data. Both points deserve a detailed study before a robust conclusion can be reached, which however is beyond the scope of this paper.

[27] Figure 8 shows the comparisons between the ECMWF analyzed temperature and the in situ data over the cold-semiarid Naqu area. Both the soil temperature analyses (i.e., ECMWF-Oper-OI and ECMWF-H-SAF) underestimated

Table 4. The Maqu Network Area – Statistics of the ECMWF Operational Run (ECMWF-Oper-OI) and the ECMWF-H-SAF Numerical Experiment (Using the EKF Soil Moisture Analysis With ASCAT Data Assimilation) Compared to In Situ Measured Soil Moisture ($m^3 \cdot m^{-3}$)

Layer Depth	RMSD (ECMWF-Oper-OI)	MD (ECMWF-Oper-OI)	*R* (ECMWF-Oper-OI)	RMSD (ECMWF- -H-SAF)	MD (ECMWF-H-SAF)	*R* (ECMWF-H-SAF)
ECMWF first layer (0–7 cm) in situ (5 cm)	0.075	0.061	0.875	0.075	0.061	0.894
ECMWF second layer (7–28 cm) in situ (20–40 cm)	0.076	0.067	0.907	0.065	0.058	0.914
ECMWF third layer (28–100 cm) in situ (80 cm)	0.067	0.058	0.866	0.049	0.044	0.856

Shown are root mean square difference (RMSD), bias (MD), and correlation coefficient (*R*).

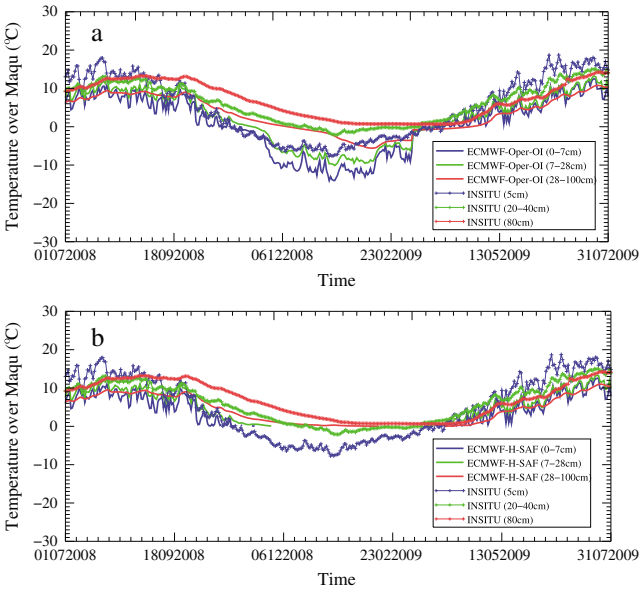

Figure 10. Same as Figure 9 but for soil temperature.

the observations at all depths, which can also be identified by the negative bias from Table 3. However, the typical daily variation patterns were captured by both analyses, which showed reasonable correlation coefficient with the observations (see Figure 8 and Table 3). The correlation between the analyses and the observations for the first layer is weaker than for the second layer. Before September 2008, both the soil temperature analyses actually have a negative correlation to the observed temperature, for the first layer. Nevertheless, the general trends of the analyses follow the observed ones. The underestimation of soil temperature can be attributed to two aspects: (1) the net heat flux into the soil (e.g., ground heat flux) and (2) the soil heat transport scheme. The first aspect is related to the calculation of surface energy partitioning of net radiation into latent heat, sensible heat and ground heat fluxes. Assuming the net incoming energy is constant, a wet soil will dissipate more energy into latent heat flux than the dry soil, which subsequently means less ground heat flux for the (modeled) wet soil. For the second aspect, ECMWF IFS fixed the quartz content typical of a loamy soil, which is around 40–60%, while the local sampled quartz content is above 85% for the Naqu network. The mismatch of thermal conductivity parameters between the model and the in situ field will definitely contribute partially to the bias. Another point worth of mentioning is the treatment of the soil freezing/thawing process in ECMWF IFS, which decoupled the soil water transport and the soil water phase changes (e.g., heat transport due to freezing/thawing) [*Viterbo et al*., 1999]. This is another possible factor partially contributing to the underestimation error of ECMWF soil temperature analysis, for this cold-semiarid Naqu network, where soil can be frozen during winter period.

[28] As can be seen from Table 3, RMSD and MD of both analyses are the highest in the first layer. With the less fluctuated soil temperature in the second layer, the ECMWF analysis performed reasonably well. Although the advantage of ECMWF-H-SAF over ECMWF-Oper-OI is infinitesimal, Table 3 shows that the EKF scheme improves the soil temperature analyses about 3.7% and 5.6% over the OI scheme (i.e., in terms of RMSD), for the first and second layer, respectively.

4.2. Results of ECMWF-Oper-OI and ECMWF-H-SAF at Maqu Network

[29] The computed soil moisture of the first three layers by the ECMWF-Oper-OI system and the ECMWF-H-SAF system are plotted with the measured soil moisture values at Maqu network in Figures 9a and 9b, for the period from 1 July 2008 to 23 September 2009, covering the whole year including the monsoon and the winter period. The in situ soil moisture is the simple average of measurements at the available stations, and the ECMWF soil moisture analyses shown here are only liquid water content.

[30] For this network, the ECMWF estimates, RMSD, bias (MD) and coefficient of correlation (R) are listed in Table 4 for the ECMWF-Oper-OI and the ECMWF-H-SAF, indicating a reasonable agreement (Figure 9). By using the EKF analysis with assimilating the ASCAT product, the results are not significantly improved (nor deteriorated) in this area, although it can be observed that some impacts were evident for all layers in the winter period from December 2008 to February 2009. The ECMWF model estimates in the first two layers follow the dynamics of the in situ measurements very well with somewhat smaller range in the monsoon period (Figure 9). A bigger deviation (underestimation up to 0.1 $m^3 \cdot m^{-3}$) is observed for the second and third layers in the winter period and an overestimation in these two layers in the monsoon period. This change of sign in the deviation (underestimation in winter and overestimation in monsoon period) may be caused by the treatment of the frozen water in winter. In the ECMWF land surface model, the water

Table 5. The Naqu Network Area - Statistics of the ECMWF Operational Run (ECMWF-Oper-OI) and the ECMWF-H-SAF Numerical Experiment (Using the EKF Soil Moisture Analysis With ASCAT Data Assimilation) Compared to the In Situ Measured Soil Temperature (°C)

Layer Depth	RMSD (ECMWF-Oper-OI)	MD (ECMWF-Oper-OI)	R (ECMWF-Oper-OI)	RMSD (ECMWF-H-SAF)	MD (ECMWF-H-SAF)	R (ECMWF-H-SAF)
ECMWF first layer (0–7 cm) in situ (5 cm)	5.03	−4.24	0.94	5.12	−4.31	0.92
ECMWF second layer (7–28 cm) in situ (20–40 cm)	4.13	−3.52	0.97	2.40	−2.19	0.97
ECMWF third layer (28–100 cm) in situ (80 cm)	3.79	−3.59	0.97	3.20	−2.91	0.97

Shown are root mean square difference (RMSD), bias (MD), and correlation coefficient (R).

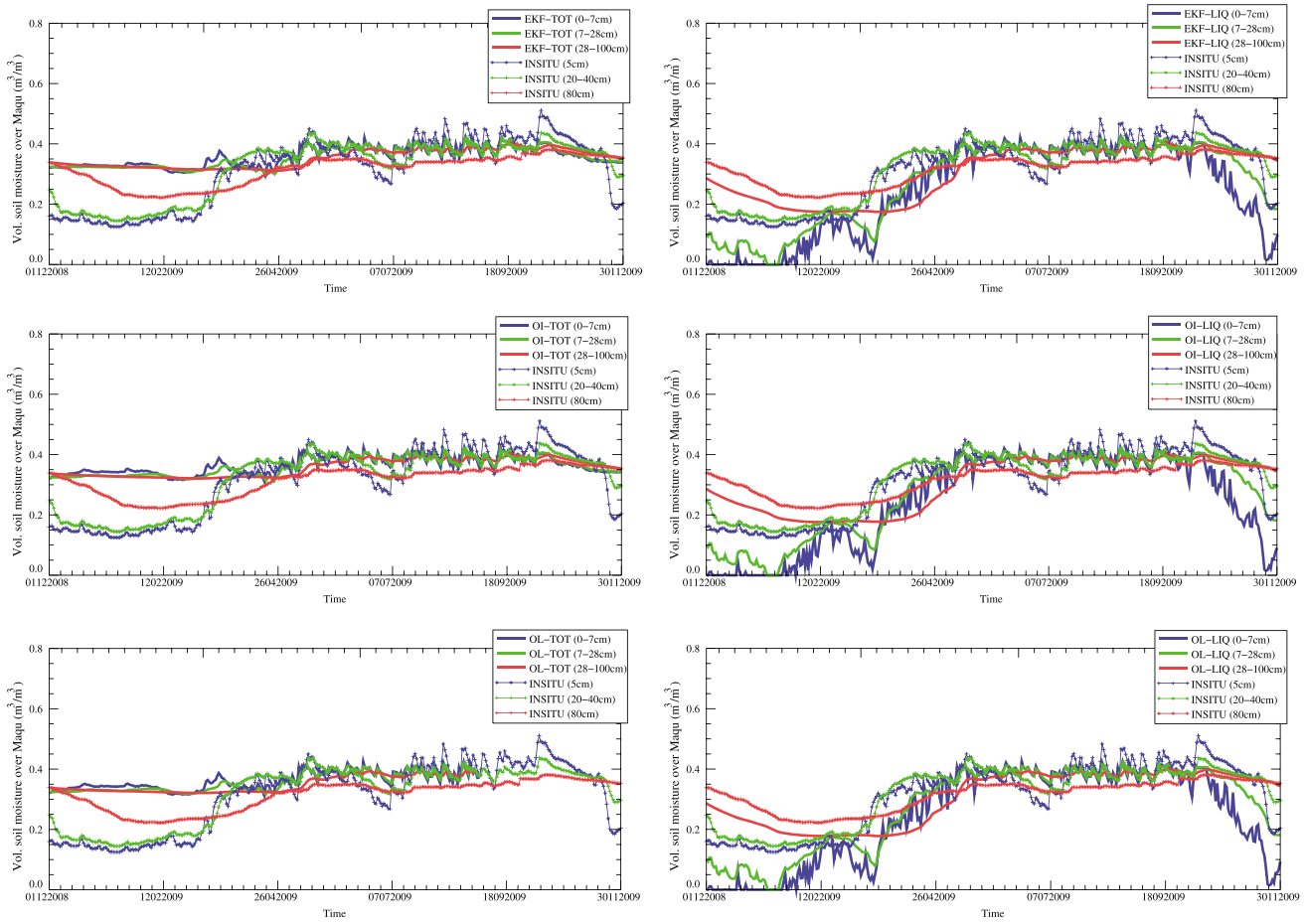

Figure 11. (a) The comparison of ECMWF soil moisture analysis for total soil moisture product ("–TOT") using screen-level proxy observation as input based on EKF scheme, OI scheme, and OL scheme for the three soil layers, with in situ observations at Maqu network. (b) The comparison of ECMWF soil moisture analysis for liquid only product ("–LIQ") using screen-level proxy observation as input based on EKF scheme, OI scheme, and OL scheme for the three soil layers, with in situ observations at Maqu network.

transport in frozen soil is limited by considering the effective hydraulic conductivity and diffusivity to be a weighted average of the value for total soil water and a very small value for frozen water (e.g., the value of the permanent wilting point) [*Viterbo et al*., 1999]. It is also realized that the higher soil moisture can be due to the spatial averaging of the in situ measurements, where some areas are frozen at certain depths while others are not (see Figure 4), compared to the homogeneous frozen model layers.

[31] Figure 10 shows the comparisons between the ECMWF analyzed temperature and the in situ data over the cold-humid Maqu area. Compared to the results in Figure 8, the ECMWF soil temperature analyses perform much better in the cold-humid area than in the cold-semiarid area, because the decreases in RMSD and MD and the increases in R can be seen in Table 5 when compared to Table 3. The performance characteristics of the soil temperature analyses in the Maqu area are similar with that in the Naqu area. The surface temperature analyses show the weakest correlation with the observations, with the highest RMSD. The EKF scheme over-performs the OI scheme about 3.5%, 42%, and 15%, in terms of RMSD. One caution here is appropriate. For the first and the second layer, the ECWMF-H-SAF does not deliver the soil temperature analyses during the whole period for the comparison (e.g., no analysis data from about 13 October 2008 to about 15 March 2009). Nevertheless, for the rest of the period, the soil temperature analyses follow the variation of the observation reasonably well. The high correlation coefficient indicates that both ECMWF soil temperature analyses have higher confidence in cold-humid area (e.g., Maqu) than in cold-semiarid area (e.g., Naqu).

4.3. Comparison of Different Analysis Methods

[32] In the above discussions, the comparison of the ECMWF-Oper-OI analysis and ECMWF-H-SAF with the in situ measurements was presented. However, no evaluation was carried out on soil moisture analysis based on OI scheme and EKF scheme without using ASCAT data, but both using only the increments of the screen-level parameters analysis as input. To carry out a complete evaluation, the comparison with Open Loop (OL, e.g., without assimilation) is also discussed here. In Figures 11a and 11b, we show the comparison between the in situ observation (e.g., Maqu station) and the soil moisture analysis. The latter one includes liquid water content only (e.g., OI-LIQ, EKF-LIQ, OL-LIQ) and

Table 6. Statistics of the Performance of ECMWF Total Soil Moisture Analysis (e.g., Liquid and Solid, "TOT") Using Screen-Level Proxy Observation as Input Based on EKF Scheme, OI Scheme, and OL Scheme, for the Three Soil Layers at Maqu Network

		RMSE	MD	*R*	*Nr*
		Overall Period			
ECMWF first layer (0–7 cm)	EKF-TOT	0.103	0.079	0.774	365
in situ (5 cm)	OI-TOT	0.109	0.082	0.738	365
	OL-TOT	0.109	0.082	0.74	365
ECMWF second layer (7–28 cm)	EKF-TOT	0.085	0.061	0.74	365
in situ (20–40 cm)	OI-TOT	0.088	0.062	0.764	365
	OL-TOT	0.088	0.062	0.767	365
ECMWF third layer (28–100 cm)	EKF-TOT	0.049	0.039	0.814	365
in situ (80 cm)	OI-TOT	0.053	0.082	0.833	365
	OL-TOT	0.052	0.043	0.837	365
		Monsoon			
ECMWF first layer (0–7 cm)	EKF-TOT	0.048	0.038	0.446	92
in situ (5 cm)	OI-TOT	0.05	0.04	0.477	92
	OL-TOT	0.049	0.039	0.443	92
ECMWF second layer (7–28 cm)	EKF-TOT	0.031	0.026	0.329	92
in situ (20–40 cm)	OI-TOT	0.0323	0.026	0.323	92
	OL-TOT	0.031	0.025	0.391	92
ECMWF third layer (28–100 cm)	EKF-TOT	0.032	0.028	0.309	92
in situ (80 cm)	OI-TOT	0.041	0.037	0.353	92
	OL-TOT	0.038	0.035	0.397	92
		Winter			
ECMWF first layer (0–7 cm)	EKF-TOT	0.179	0.178	−0.564	90
in situ (5 cm)	OI-TOT	0.191	0.19	−0.627	90
	OL-TOT	0.191	0.19	−0.619	90
ECMWF second layer (7–28 cm)	EKF-TOT	0.154	0.153	−0.246	90
in situ (20–40 cm)	OI-TOT	0.161	0.159	−0.537	90
	OL-TOT	0.161	0.159	−0.551	90
ECMWF third layer (28–100 cm)	EKF-TOT	0.072	0.064	0.913	90
in situ (80 cm)	OI-TOT	0.075	0.067	0.947	90
	OL-TOT	0.075	0.067	0.944	90

RMSE: root mean square error; MD: bias; *R*: correlation coefficient; *Nr*: number of values used.

Table 7. Same as Table 6 but for Liquid Soil Moisture

		RMSE	MD	*R*	*Nr*
		Overall Period			
ECMWF first layer (0–7 cm)	EKF-LIQ	0.102	0.083	0.88	365
in situ (5 cm)	OI-LIQ	0.101	0.052	0.878	365
	OL-LIQ	0.101	0.082	0.879	365
ECMWF second layer (7–28 cm)	EKF-LIQ	0.072	0.054	0.932	365
in situ (20–40 cm)	OI-LIQ	0.07	0.043	0.933	365
	OL-LIQ	0.069	0.051	0.934	365
ECMWF third layer (28–100 cm)	EKF-LIQ	0.048	0.042	0.931	365
in situ (80 cm)	OI-LIQ	0.048	0.042	0.929	365
	OL-LIQ	0.047	0.042	0.932	365
		Monsoon			
ECMWF first layer (0–7 cm)	EKF-LIQ	0.045	0.041	0.301	92
in situ (5 cm)	OI-LIQ	0.052	0.042	0.298	92
	OL-LIQ	0.051	0.042	0.3	92
ECMWF second layer (7–28 cm)	EKF-LIQ	0.031	0.026	0.329	92
in situ (20–40 cm)	OI-LIQ	0.033	0.026	0.323	92
	OL-LIQ	0.031	0.025	0.391	92
ECMWF third layer (28–100 cm)	EKF-LIQ	0.037	0.033	0.363	92
in situ (80 cm)	OI-LIQ	0.043	0.04	0.395	92
	OL-LIQ	0.041	0.038	0.422	92
		Winter			
ECMWF first layer (0–7 cm)	EKF-LIQ	0.117	0.106	0.584	90
in situ (5 cm)	OI-LIQ	0.117	0.106	0.587	90
	OL-LIQ	0.116	0.105	0.587	90
ECMWF second layer (7–28 cm)	EKF-LIQ	0.098	0.087	0.529	90
in situ (20–40 cm)	OI-LIQ	0.097	0.086	0.522	90
	OL-LIQ	0.096	0.084	0.52	90
ECMWF third layer (28–100 cm)	EKF-LIQ	0.054	0.054	0.992	90
in situ (80 cm)	OI-LIQ	0.053	0.053	0.993	90
	OL-LIQ	0.052	0.052	0.99	90

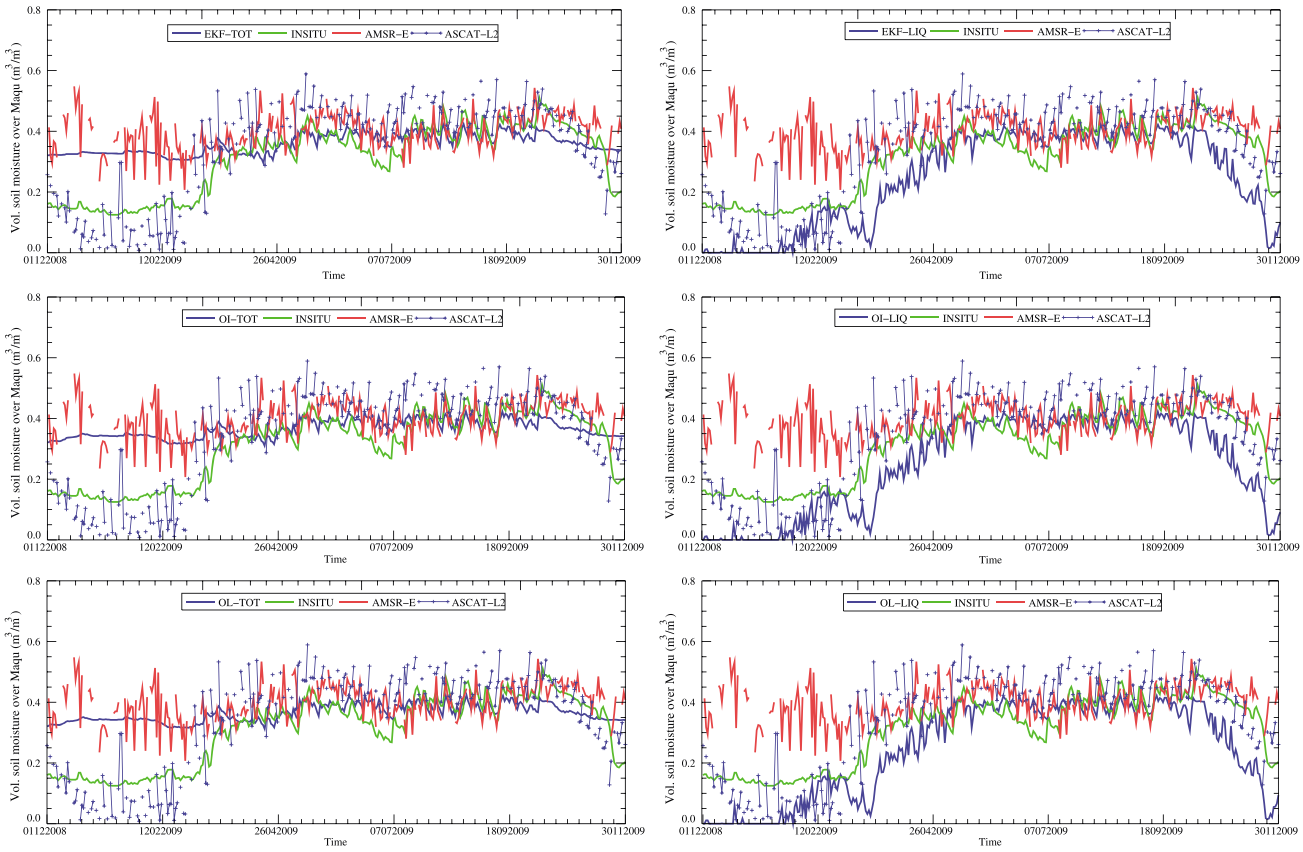

Figure 12. (a) Comparison among the ECMWF's surface soil moisture analysis for total soil moisture product ("–TOT"), the ASCAT-L2 data, the AMSR-E data and the in situ data for the first soil layer (5 cm) at Maqu Network. (b) Comparison among the ECMWF's surface soil moisture analysis for liquid only product ("–LIQ"), the ASCAT-L2 data, the AMSR-E data and the in situ data for the first soil layer (5 cm) at Maqu Network.

both liquid and solid water content (e.g., OI-TOT, EKF-TOT, OL-TOT), based on OI, EKF, and OL scheme, from 1 December 2008 to 30 November 2009 (e.g., from the winter period to the monsoon period). It is evident that the soil moisture analysis excluding the solid water content outperforms the analysis including both liquid and solid water content, when compared to in situ observations. This can be explained by that the ground measurements sensors rely on dielectric constant measurements, which are related to the liquid soil moisture content and variations (i.e., not to the solid water content). This explains why only the liquid soil moisture analysis is shown in Figures 7 and 9.

[33] Tables 6 and 7 list the statistics (e.g., RMSE, MD, and R) for the comparison implemented for the total moisture analysis and the liquid only moisture analysis. The statistics for the liquid only product shows an overall improved performance. Especially for the comparison during the winter period, the correlation coefficients for the first two soil layers change from negative to positive, which indicate a dramatic improvement in terms of performance of the soil moisture analysis (Figure 11). For all three soil layers, Figure 11 shows that ECMWF soil moisture analysis underestimates the in situ observations during the winter period and overestimates during the monsoon period, which follows the pattern shown in Figure 9. This pattern is more evident for the third soil layer, compared to other layers. One possible explanation is that due to the treatment of soil moisture transport in frozen soil in ECMWF IFS, the hydraulic conductivity and diffusivity have been semiempirically reduced with a weighted factor, for which the ECMWF soil property, here at 80 km resolution, is not representative of the local soil property. In addition, the strength of the local soil-vegetation-atmosphere coupling is weakest in the third soil layer. This is the reason that the phase shift can be clearly identified for the third soil layer in Figure 11.

[34] From Figure 11, there are no significant differences in soil moisture analysis based on different schemes. However, the analysis based on the EKF scheme does make the ECMWF estimations closer to the in situ observations than the OL scheme, in terms of RMSE and MD values. For the comparison between the analysis based on OI scheme and OL scheme, there is no change or slight deterioration can be found (Tables 6 and 7). When only liquid soil moisture analysis is used, no clear difference can be identified among the soil moisture analysis based on different schemes, although a negligible better performance can be identified for the soil moisture analysis based on the EKF scheme for the monsoon period, compared to the other two schemes. Nevertheless, Table 7 shows that R for the first and second layer during winter period turns positive, indicating that the

Table 8. Statistics of the Performance of ECMWF Analysis Based on EKF Scheme, OI Scheme, and OL Scheme, for the First Soil Layer (0–0.05 m) at Maqu Network, in Terms of Comparison With Satellite Data (AMSR-E and ASCAT-L2)

			RMSE	MD	*R*	*Nr*
		EKF				
Overall period	EKF-TOT	AMSR-E	0.072	0.057	0.315	309
		ASCAT-L2	0.142	0.113	***0.718***	247
	EKF-LIQ	AMSR-E	0.211	0.157	0.25	309
		ASCAT-L2	0.134	0.107	***0.833***	247
Winter	EKF-TOT	AMSR-E	0.097	0.079	−0.269	72
		ASCAT-L2	0.24	0.228	−0.122	60
	EKF-LIQ	AMSR-E	0.355	0.338	−0.315	72
		ASCAT-L2	0.107	0.085	−0.105	60
Monsoon	EKF-TOT	AMSR-E	0.056	0.043	0.115	80
		ASCAT-L2	0.087	0.072	0.203	61
	EKF-LIQ	AMSR-E	0.058	0.045	0.036	80
		ASCAT-L2	0.088	0.074	0.182	61
		OI				
Overall period	OI-TOT	AMSR-E	0.068	0.054	0.298	309
		ASCAT-L2	0.146	0.114	***0.697***	247
	OI-LIQ	AMSR-E	0.21	0.156	0.245	309
		ASCAT-L2	0.133	0.105	***0.832***	247
Winter	OI-TOT	AMSR-E	0.09	0.074	−0.247	72
		ASCAT-L2	0.252	0.241	−0.215	60
	OI-LIQ	AMSR-E	0.355	0.337	−0.32	72
		ASCAT-L2	0.11	0.085	−0.102	60
Monsoon	OI-TOT	AMSR-E	0.054	0.042	0.079	80
		ASCAT-L2	0.082	0.247	0.067	61
	OI-LIQ	AMSR-E	0.057	0.044	−0.013	80
		ASCAT-L2	0.083	0.069	0.204	61
		OL				
Overall period	OL-TOT	AMSR-E	0.068	0.054	0.315	309
		ASCAT-L2	0.146	0.114	***0.687***	247
	OL-LIQ	AMSR-E	0.21	0.155	0.246	309
		ASCAT-L2	0.132	0.105	***0.833***	247
Winter	OL-TOT	AMSR-E	0.09	0.074	0.264	72
		ASCAT-L2	0.252	0.241	−0.22	60
	OL-LIQ	AMSR-E	0.354	0.336	−0.325	72
		ASCAT-L2	0.11	0.085	−0.11	60
Monsoon	OL-TOT	AMSR-E	0.054	0.043	0.131	80
		ASCAT-L2	0.084	0.069	0.157	61
	OL-LIQ	AMSR-E	0.057	0.044	0.042	80
		ASCAT-L2	0.086	0.071	0.143	61

RMSE: root mean square error; MD: bias; *R*: correlation coefficient; *Nr*: number of values used.

analysis should be performed for the liquid water content only rather than the total soil moisture in winter period to better utilize the in situ observations in evaluating the different analyses.

4.4. Surface Analyses Against Satellite Data

[35] In Figure 12, we show the comparison among the operational satellite data [*Su et al*., 2011], the in situ data, and the ECMWF's surface soil moisture analysis (e.g., the first soil layer, 0–0.07 m). The results show that the ECMWF's liquid only surface analysis is in good agreement with both the in situ observations and the satellite observations (e.g., ASCAT-L2 data). For the total (liquid plus solid) soil moisture analysis, although the ECMWF surface analysis dramatically overestimates the in situ observations, it is mostly in the variation range of the AMSR-E data (Figure 12). This implies that AMSR-E soil moisture data may be contaminated by the frozen soil, which needs further investigation. For the liquid only soil moisture analysis, the ECMWF surface analysis underestimates the in situ observations as the above discussion mentioned. However, it follows the general variation of ASCAT-L2 soil moisture data with a high correlation coefficient (Figure 12).

[36] There are no significant differences in soil moisture analyses derived from different schemes. The statistics (e.g., RMSE, MD, and *R*) between the satellite data and the ECMWF surface moisture analysis are given in Table 8. The RMSE and MD values between the EKF-TOT and the AMSR-E are much smaller than those between the EKF-TOT and the ASCAT-L2. It seems that the EKF-TOT can better match with the AMSR-E data than with the ASCAT-L2. However, there is no strong correlation between the EKF-TOT surface soil moisture analysis and the AMSR-E data, although the analysis lies in the variation range of AMSR-E data. On the other hand, although the EKF-TOT analysis dramatically overestimates the ASCAT-L2 data during the winter, it can follow the variability of ASCAT-L2 data as the high correlation coefficient (0.718) indicates. For liquid only analysis, there is a higher correlation coefficient (0.833) than the total soil moisture analysis does, due to the elimination of contamination by frozen soil. For all the three different schemes, the higher correlation between the ECMWF surface analysis (including both the total and the liquid only soil moisture analysis) and the ASCAT-L2 data exists (e.g., the highlighted value in Table 8), compared to the correlation between the analysis and the AMSR-E data. From Table 8,

no robust results can be reached when it is specified with the winter period or the monsoon period. Especially for the winter period, no correlation between the ECMWF surface analysis and the satellite data can be identified (e.g., almost all correlation coefficients during the winter period are negative, and the absolute value less than 0.4).

5. Conclusions

[37] Using in situ measurements from two newly established regional soil moisture and soil temperature networks on the Tibetan Plateau, we have conducted an evaluation on the previous ECMWF operational land surface analysis system using an OI scheme and the current system based on a point-wise extended-Kalman filter scheme. The latter scheme produces soil moisture analysis derived from the screen-level parameter analysis only and from both the screen-level analysis and ASCAT data. For the first time, the evaluation on the ECMWF soil moisture analysis is carried out for two hydrologically contrasting but thermodynamically similar areas on the Tibetan Plateau, one cold-semiarid and one cold-humid area. The analysis aims to understand the ability or deficiency of the land surface analysis scheme in the ECMWF IFS.

[38] For the cold-semiarid Naqu area, the ECMWF model overestimates significantly the regional soil moisture in the monsoon seasons. The overestimation may be caused by the used soil texture information (e.g., from the standard FAO texture information) and adapted to the IFS soil texture classes, which may not be representative for the Tibetan Plateau [*Albergel et al*., 2010]. Further improvements might be obtained by a better representation of soil texture. For example, the implementation of a new map such as the new comprehensive Harmonized World Soil Database (FAO, 2009) could lead to better results [*Albergel et al*., 2012a, 2012b]. For the cold-humid Maqu network area, the ECMWF products have comparable accuracy as reported by previous studies in the humid monsoon period. The ECMWF EKF-TOT products, which include solid and liquid water contents, overestimate the soil moisture over the area in the winter period significantly. However, this discrepancy can be reconciled when only the liquid water content is analyzed with the in situ measurements. For the soil temperature, the ECMWF analyses perform better in the cold-humid area (e.g., Maqu) than in the cold-semiarid area (e.g., Naqu).

[39] To make a fair comparison among the in situ data, the remote sensing data and the ECMWF soil moisture products, for the cold-humid Maqu network, the soil moisture analyses based on EKF, OI, and OL scheme were derived by using the screen-level proxy observations only. Two comparisons were made: one for the in situ observations, the other for the satellite data. For the in situ data case, ECMWF's analyses from the three soil layers were compared with the corresponding observations. The comparison reinforces that the discrepancy between the EKF-TOT analysis and the in situ data can be reconciled when only the liquid water content is analyzed. It is found that the liquid only soil moisture analysis based on EKF does outperform the other two schemes, when compared with the in situ observations. For the comparison between the analysis based on OI scheme and OL scheme, there is no change or slight deterioration can be found. For the satellite data case, the higher correlation between the ECMWF surface analysis and the ASCAT-L2 data were found existing for all three different schemes. However, no robust results can be reached when it is specified with the winter period or the monsoon period separately.

[40] In summary, the current operational soil moisture analysis at ECMWF has comparable accuracy in regards to the in situ observations at Maqu network, which is a cold and humid area on the Tibetan Plateau. For the cold and semiarid area on the Tibetan Plateau, further improvement of the ECMWF land surface model and soil texture parameter database is needed, to reduce the tendency of overestimating the model soil moisture field. The recently accomplished soil moisture and soil temperature observation network at Ngari station on the Tibetan Plateau [*Su et al*. 2011], in a cold-arid environment, can be used to validate any further improvement of the land surface model. The soil moisture analysis with assimilating ASCAT data does not significantly improve the performance of the analysis, due to the CDF-matching approach used and partially due to the data quality. The recent improvements in the ASCAT soil moisture products and bias correction are expected to enhance the impact of using ASCAT in the soil moisture analysis. With the current ECMWF land surface analysis scheme, it is expected that the new satellite surface products, such as those from the Soil Moisture and Ocean Salinity satellite, and the Soil Moisture Active and Passive satellite can be assimilated to improve the performance of the current operational surface products.

[41] **Acknowledgments.** This work was funded in part by the ESA-MOST Dragon I/II programme (Drought Monitoring, Prediction and Adaptation under Climatic Changes project and Young Scientists Support), and the European Commission (Call FP7-ENV-2007-1 grant 212921) CEOP – AEGIS project (http://www.ceop-aegis.org/). The ECMWF soil moisture product using ASCAT data assimilation was produced in the framework of the EUMETSAT H-SAF project. We thank Albergel for his comments on the paper, and we thank all other participating colleagues and students for their contributions to the data collection campaigns.

References

Albergel, C., et al. (2010), Cross-evaluation of modelled and remotely sensed surface soil moisture with in situ data in southwestern France, *Hydrol. and Earth Syst. Sci.*, *14*, 2177–2191.

Albergel C., P. de Rosnay, G. Balsamo, L. Isaksen, and J. Muñoz Sabater (2012a), Soil moisture analyses at ECMWF: Evaluation using global ground-based in situ observations, *J. Hydrometeorol.*, *13*, 1442–1460.

Albergel C., P. de Rosnay, C. Gruhier, J. Muñoz Sabater, S. Hasenauer, L. Isaksen, Y. Kerr, and W. Wagner (2012b), Evaluation of remotely sensed and modelled soil moisture products using global ground-based in-situ observations, *Remote Sens. Environ.*, *118*, 215–226, doi:10.1016/j.rse.2011.11.017.

Balsamo, G., P. Viterbo, A. Beljaars, B. van den Hurk, M. Hirschi, A. K. Betts, and K. Scipal, (2009), A revised hydrology for the ECMWF model: verification from field site to terrestrial water storage and impact in the Integrated Forecast System, *J. Hydrometeorol.*, *10*, 623–643.

Bartalis, Z., W. Wagner, V. Naeimi, S. Hasenauer, K. Scipal, H. Bonekamp, J. Figa, and C. Anderson (2007), Initial soil moisture retrievals from the METOP-A Advanced Scatterometer (ASCAT), *Geophys. Res. Lett.*, *34*, L20401, doi:10.1029/2007GL031088.

Bengtsson, L. (2010), The global atmospheric water cycle, *Environ. Res. Lett.*, *5*, doi:10.1088/1748-9326/5/2/025002.

Chen, Y., K. Yang, W. Tang, J. Qin, and L. Zhao (2012), Parameterizing soil organic carbon's impact on soil porosity and thermal parameters for Eastern Tibet grasslands, *Science China Earth Sciences*, *55*(6), 1001–1011, doi:10.1007/s11430-012-4433-0.

Dee, D. P., et al. (2011), The ERA-Interim reanalysis: configuration and performance of the data assimilation system, *Q. J. R. Meteorol. Soc. 137*, 553–597, doi:10.1002/qj.828.

de Rosnay P., M. Drusch, A. Boone, G. Balsamo, B. Decharme, P. Harris, Y. Kerr, T. Pellarin, J. Polcher, and J.-P. Wigneron (2009), The AMMA Land Surface Model Intercomparison Experiment coupled to the Community Microwave Emission Model: ALMIP-MEM, *J. Geophys. Res.*, *114*, D05108, doi:10.1029/2008JD010724.

de Rosnay, P., G. Balsamo, C. Albergel, J. Muñoz-Sabater, and L. Isaksen (2012a), Initialisation of land surface variables for Numerical Weather Prediction, *Surv. Geophys.*, in press, doi:10.1007/s10712-012-9207-x Print ISSN 0169-3298 Online ISSN 1573-0956.

de Rosnay P., M. Drusch, D. Vasiljevic, G. Balsamo, C. Albergel, and L. Isaksen, (2012b), A simplified Extended Kalman Filter for the global operational soil moisture analysis at ECMWF, *Q. J. R. Meteorol. Soc*, doi:10.1002/qj.2023.

Dente, L., Z. Vekerdy, Z. Su, and J. Wen (2009), Continuous in situ soil moisture measurements at Maqu site, Tech. rep., EU CEOP AEGIS project, 12, pp. ITC, Enschede.

Dente, L., Z. Vekerdy, Z. Su, and J. Wen (2011), Maqu network for validation of satellite–derived soil moisture products, *Inter. J. App. Earth Obs. and Geo-information*, *17*, 55–65.

Dirmeyer, P. A., Z. C. Guo, and X. Gao (2004), Comparison, validation, and transferability of eight multiyear global soil wetness products, *J. Hydrometeorol.*, *5*(6), 1011–1033.

Dorigo, W., K. Scipal, R. Parinussa, Y. Y. Liu, W. Wagner, R. De Jeu, and V. Naeimi (2010), Error characterization of global active and passive microwave soil moisture data sets, *Hydrol. Earth Syst. Sci.*, *14*, 2605–2616, doi:10.5194/hess-14-2605-2010. (Special Issue: Earth observation and water cycle science).

Drusch, M. (2007), Initializing numerical weather prediction models with satellite-derived surface soil moisture: Data assimilation experiments with ECMWF's Integrated Forecast System and the TMI soil moisture data set, *J. Geophys. Res.*, *112*, D03102, doi:10.1029/2006JD007478.

Drusch, M., and P. Viterbo (2007), Assimilation of screen-level variables in ECMWF's Integrated Forecast System: A study on the impact on the forecast quality and analysed soil moisture, *Mon. Wea. Rev.*, *135*, 300–314.

Drusch, M., E. F. Wood, and H. Gao (2005), Observation operators for the direct assimilation of TRMM microwave imager retrieved soil moisture, *Geophys. Res. Lett.*, *32*, L15403, doi:10.1029/2005GL023623.

Drusch, M., K. Scipal, P. de Rosnay, G. Balsamo, E. Andersson, P. Bougeault, and P. Viterbo (2009), Towards a Kalman Filter based soil moisture analysis system for the operational ECMWF Integrated Forecast System, *Geophys. Res. Lett.*, *36*, L10401, doi:10.1029/2009GL037716.

Ma, Y., J. M. Wang, R. H. Huang, G. Wei, M. Menenti, Z. Su, Z. Y. Hu, F. Gao, and J. Wen (2003), Remote sensing parameterization of land surface heat fluxes over arid and semi-arid areas, *Adv. Atmosph. Res.*, *20*(4), 530–539.

Ma, Y., L. Zhong, Z. Su, H. Ishikawa, M. Menenti, and T. Koike (2006), Determination of regional distributions and seasonal variations of land surface heat fluxes from Landsat-7 Enhanced Thematic Mapper data over the central Tibetan Plateau area, *J. Geophys. Res.*, *111*, D10305, doi:10.1029/2005JD006742.

Ma, Y., M. Song, H. Ishikawa, K. Yang, T. Koike, L. Jia, M. Menenti, and Z. Su (2007), Estimation of the regional evaporative fraction over the Tibetan Plateau area by using Landsat-7 ETM data and the field observations, *J.Meteorological Soc. Japan*, *85A*, 295–309.

Mahfouf, J.-F., P. Viterbo, H. Douville, A. C. M. Beljaars, and S. Saarinen (2000), A revised land-surface analysis scheme in the Intergrated Forecasting System, ECMWF Newsletter No. 88,8-13, http://www.ecmwf.int/publications/newsletters/pdf/88.pdf.

Milly, P. C. D., and K. A. Dunne (1994), Sensitivity of the global water cycle to the water-holding capacity of land, *J. Climate*, *7*, 506–526.

Njoku, E. G., T. J. Jackson, V. Lakshmi, T. K. Chan, and S. V. Nghiem (2003), Soil moisture retrieval from AMSR-E, *IEEE Trans. Geosci. Remote Sens.*, *41*, 215–229.

Owe, M., R. De Jeu, and T. Holmes (2008), Multisensor historical climatology of satellite-derived global land surface moisture, *J. Geophys. Res.*, *113*, F01002, doi:10.1029/2007JF000769.

Polcher, J. (1995), Sensitivity of tropical convection to land surface processes. *J. Atmos. Sci.*, *52*, 3144–3161.

Qin, J., S. L. Liang, K. Yang, I. Kaihotsu, R. G. Liu, and T. Koike (2009), Simultaneous estimation of both soil moisture and model parameters using particle filtering method through the assimilation of microwave signal, *J. Geophys. Res.*, *114*, D15103, doi:10.1029/2008JD011358.

Reynolds, C. A., T. J. Jackson, and W. J. Rawls, Estimating Available Water Content by Linking the FAO Soil Map of the World with Global Soil Profile Databases and Pedo-transfer Functions. Proceedings of the AGU 1999 Spring, Conference, Boston, MA. 1 May-4 June, 1999.

Scipal, K., T. Holmes, R. De Jeu, V. Naeimi, and W. Wagner (2008), A possible solution for the problem of estimating the error structure of global soil moisture data sets, *Geophys. Res. Lett.*, *35*, L24403, doi:10.1029/2008GL035599.

Su, Z., J. Wen, L. Dente, R. van der Velde, L. Wang, Y. Ma, K. Yang, and Z. Hu (2011), The Tibetan Plateau observatory of plateau scale soil moisture and soil temperature (Tibet-Obs) for quantifying uncertainties in coarse resolution satellite and model products, *Hydrol. Earth Syst. Sci.*, *15*, 2303–2316, doi:10.5194/hess-15-2303-2011.

Tian, X. J., Z.-H. Xie, A. G. Dai, C. X. Shi, B. H. Jia, F. Chen, and K. Yang (2009), A dual-pass variational data assimilation framework for estimating soil moisture profiles from AMSR-E microwave brightness temperature, *J. Geophys. Res.*, *114*, D16102, doi:10.1029/2008JD011600.

van der Velde, R. (2010), Soil moisture remote sensing using active microwaves and land surface modelling, PhD thesis, University of Twente, Enschede, the Netherlands, 193 pp.

van der Velde, R., and Z. Su (2009), Dynamics in land surface conditions on the Tibetan Plateau observed by ASAR, *Hydrol. Sci. J.*, *54*(6), 1079–1093.

van der Velde, R., Z. Su, and Y. Ma (2008), Impact of soil moisture dynamics on ASAR signatures and its spatial variability observed over the Tibetan plateau, *Sensors*, *8*, 5479–5491.

van der Velde, R., Z. Su, M. Ek, M. Rodell, and Y. Ma, Y (2009), Influence of thermodynamic soil and vegetation parameterizations on the simulation of soil temperature states and surface fluxes by the Noah LSM over a Tibetan plateau site, *Hydrol. Earth Sys. Sci.*, *13*, 759–777.

Viterbo P., and A. C. M. Beljaars (1995), An improved land surface parameterization scheme in the ECMWF model and its validation, *J. Climate*, *8*, 2716–2748.

Viterbo P., A. C. M. Beljaars, J.-F. Mahouf, and J. Teixeira (1999), The representation of soil moisture freezing and its impact on the stable boundary layer, *Q.J.R. Meteorol. Soc.*, *125*, 2401–2426.

Wagner, W., K. Scipal, C. Pathe, D. Gerten, W. Lucht, and B. Rudolf (2003), Evaluation of the agreement between the first global remotely sensed soil moisture data with model and precipitation data, *J. Geophys. Res.*, 108 (D19), D194611, doi:10.1029/2003JD003663.

Wen J., Z. B. Su, and Y. M. Ma (2003), Determination of land surface temperature and soil moisture from Tropical Rainfall Measuring Mission/Microwave Imager remote sensing data. *J. of Geophys. Res.*, *108*(D2), 4038, doi:10.1029/2002JD002176.

Wen, J., and Z. Su (2003a), A time series based method for estimating relative soil moisture with ESA wind scatterometer data, *Geophys. Res. Lett.*, *30*(7), 1397, doi:10.1029/ 2002GL016557.

Wen, J., and Z. Su (2003b), Estimation of soil moisture from ESA Windscatterometer data, *Phys. Chem. Earth*, *28*(1–3), 53–61.

Yang, K., T. Koike, I. Kaihotsu, and J. Qin (2009), Validation of a dual-pass microwave land data assimilation system for estimating surface soil moisture in semi-arid regions, *J. Hydrometeorol.*, *10*(3), 780–794.

Yoshikawa, K., and P. Overduin (2005), Comparing unfrozen water content measurements of frozen soil using recently developed commercial sensors, *Cold Regions Sci. and Tech.*, *42*, 250–256.